Passive Scalars in Stratified Turbulence

G. Brethouwer

Linné Flow Centre, KTH Mechanics, SE-100 44 Stockholm, Sweden

E. Lindborg

Linné Flow Centre, KTH Mechanics, SE-100 44 Stockholm, Sweden

---

G. Brethouwer, Linné Flow Centre, KTH Mechanics, SE-100 44 Stockholm, Sweden. (geert@mech.kth.se)

E. Lindborg, Linné Flow Centre, KTH Mechanics, SE-100 44 Stockholm, Sweden. (erikl@mech.kth.se)

Statistics of a passive scalar (or tracer) with a horizontal mean gradient in randomly forced and strongly stratified turbulence are investigated by numerical simulations. We observe that horizontal isotropy of the passive scalar spectrum is satisfied in the inertial range. The spectrum has the form $E_\theta(k_h) = C_\theta \varepsilon_\theta \varepsilon_K^{-1/3} k_h^{-5/3}$, where $\varepsilon_\theta, \varepsilon_K$ are the dissipation of scalar variance and kinetic energy respectively, and $C_\theta \simeq 0.5$ is a constant. This spectrum is consistent with atmospheric measurements in the mesoscale range with wavelengths $1-500$ km. We also calculate the fourth-order passive scalar structure function and show that intermittency effects are present in stratified turbulence.

1. Introduction

To gain insight into tracer mixing in geophysical flows, we explore passive scalar statistics in strongly stratified fluids. First we consider some basic phenomenology of passive scalars statistics in isotropic turbulence. According to the Obukhov-Corrsin theory of locally isotropic turbulence, there is an inertial range in which the one-dimensional wavenumber spectrum of the variance of a passive scalar fluctuation θ has the form (Warhaft 2000)

$$E_\theta(k) = C_\theta \varepsilon_\theta \varepsilon_K^{-1/3} k^{-5/3}\,, \tag{1}$$

where ε_θ and ε_K are the dissipation of scalar variance and kinetic energy respectively and C_θ is the Obukhov-Corrsin constant. In the corresponding range of separations, r, the passive scalar structure function of an arbitrary order n, and the second-order structure function in particular, are given by

$$\langle \delta\theta^n \rangle \;\propto\; r^{n/3}\,, \tag{2}$$

$$\langle \delta\theta\delta\theta \rangle \;=\; C'_\theta \varepsilon_\theta \varepsilon_K^{-1/3} r^{2/3}\,, \tag{3}$$

where $\delta\theta = \theta' - \theta$ is the difference between the scalar values at two points separated by a vector $\boldsymbol{r}$, $\langle\rangle$ denotes an ensemble average, and $C'_\theta = 4\pi\, C_\theta/[\sqrt{3}\,\Gamma\left(\frac{5}{3}\right)] \approx 4.0\, C_\theta$. In Kolmogorov turbulence the passive scalar spectrum (1) and the second-order structure function (3) have been measured in several studies (Sreenivasan 1996, Warhaft 2000). Horizontal spectra (Nastrom *et al.* 1986, Strahan & Mahlman 1994, Tjemkes & Visser 1994, Bacmeister *et al.* 1996, Cho *et al.* 1999) and second-order structure functions (Lindborg & Cho 2000, Sparling & Bacmeister 2001) of passive tracers measured in the mesoscale range ($1 - 500$ km) of the middle atmosphere appear to have the same functional form as

(1) and (3). However, the similarity between the measured spectra and the second-order structure functions and the theoretical expressions (1) and (3) can not be explained by the classical Obukhov-Corrsin theory, which is based on the assumption of local isotropy. The isotropy assumption would imply that we should be able to measure a vertical spectrum of the same form as the horizontal spectrum in the wavelength range $1 - 500$ km. For obvious reasons this cannot be true and we must look for another explanation.

Nastrom *et al.* (1986) and Tjemkes & Visser (1994) suggested that the scalar spectra originate from mixing in two-dimensional turbulence, but mixing by gravity waves has also been mentioned as an explanation (e.g. Cho *et al.* 1999). The observed horizontal $k_h^{-5/3}$-scalar spectra may thus be explained by different dynamical processes, but, in agreement with our opinion, Bacmeister *et al.* (1996) concluded that neither two-dimensional turbulence nor gravity waves can satisfactorily explain the measurements. Therefore, we suggest an alternative explanation.

In strongly stratified fluids, large horizontal quasi two-dimensional structures are commonly observed. In recent work (Billant & Chomaz 2001, Lindborg 2006) it has been suggested that structures with characteristic horizontal length scale l_h split up into layers with characteristic thickness $l_v \sim F_h l_h$, where $F_h = U/N l_h$ is a Froude number based on the horizontal length scale, a characteristic horizontal velocity scale U and the Brunt-Väisälä frequency N. The thin layers or pancake-like structures will break up into smaller structures. Lindborg (2006) and Brethouwer *et al.* (2007) argued that this nonlinear process can repeat itself in many steps and lead to a three-dimensional strongly anisotropic energy cascade in which energy is transferred from large to small scales, as in three-dimensional turbulence. This particular type of dynamics has been observed in simulations (Riley & deBruynKops 2003; Lindborg 2006; Brethouwer *et al.* 2007; Lindborg & Brethouwer 2007). In the inertial range, the horizontal one-dimensional kinetic and potential energy spectra of stratified turbulence have the form

$$E_K(k_h) = C_K \varepsilon_K^{2/3} k_h^{-5/3}, \tag{4}$$

$$E_P(k_h) = C_P \varepsilon_P \varepsilon_K^{-1/3} k_h^{-5/3}, \tag{5}$$

where k_h is the horizontal wave number and ε_P is the potential energy dissipation. The spectra from the stratified turbulence simulations of Lindborg (2005; 2006) with and without system rotation showed a very good agreement with (4) and (5), with $C_K \simeq C_P \simeq 0.5$, and also agreed with mesoscale atmospheric horizontal $k_h^{-5/3}$-spectra measured by Nastrom & Gage (1985).

The equation for the passive scalar fluctuations with a constant mean vertical gradient has the same form as the equation for potential temperature fluctuations in a fluid with constant background stratification. In this case, the passive scalar spectrum should therefore be of the same form as in (5), which is also similar to the Obukhov-Corrsin expression (1). Moreover, the two constants, C_θ and C_P, should have the same value. It can be expected that this spectral form has a certain degree of universality, so that it can be observed in other cases, *e.g.* when the mean passive scalar gradient is in a horizontal direction. In this paper, we study the passive scalar dynamics in stratified turbulence with a constant horizontal mean gradient. To analyse whether the passive scalar spectrum is consistent with (1) it is not sufficient to verify the $k_h^{-5/3}$ dependence, since this can arise in more circumstances (Warhaft 2000). We must also study the scaling with the parameters

ε_K and ε_θ. By calculating passive scalar one-dimensional spectra and structure functions in the direction which is either aligned or perpendicular to the mean gradient we assess if the passive scalar dynamics is horizontally isotropic in the inertial range. Furthermore, we will study scalar intermittency by calculating the fourth-order passive scalar structure functions.

2. Simulations

Numerical simulations of homogeneous turbulence with a uniform stratification are carried out with a pseudospectral code using periodic boundary conditions in all three directions. The horizontal sides of the domain, L_x and L_y, are equal and much larger than the vertical side L_z (Lindborg 2005; 2006). The following set of equations are solved

$$\frac{\partial \boldsymbol{u}}{\partial t} + \boldsymbol{u}\cdot\nabla\boldsymbol{u} = -\nabla p + D_u\boldsymbol{u} + N\boldsymbol{e}_z\phi - f_o\boldsymbol{e}_z \times \boldsymbol{u} + \boldsymbol{f}, \tag{6}$$

$$\nabla\cdot\boldsymbol{u} = 0\,, \tag{7}$$

$$\frac{\partial \phi}{\partial t} + \boldsymbol{u}\cdot\nabla\phi = D_\phi\phi - Nu_z\,, \tag{8}$$

$$\frac{\partial \theta}{\partial t} + \boldsymbol{u}\cdot\nabla\theta = D_\theta\theta - \boldsymbol{G}\cdot\boldsymbol{u}. \tag{9}$$

Here, $\boldsymbol{u}$ is the velocity and u_z is the vertical velocity component, $\boldsymbol{e}_z$ is the vertical unit vector, $\phi = gT'/(NT_0)$, where T' and T_0 are the fluctuating and equilibrium potential temperature respectively, g is the gravity constant, p is the pressure, $f_o = 2\Omega\sin\sigma$ is the Coriolis parameter with σ the latitude and Ω the Earth's rotation rate, $\boldsymbol{f}$ is a forcing term, $\boldsymbol{G}$ is a mean scalar gradient, taken in the horizontal x-direction here, and D_u, D_ϕ, D_θ are diffusion operators. The latter are defined as

$$D_u = D_\phi = D_\theta = -\nu_h\nabla_h^4 - \nu_v\frac{\partial^8}{\partial z^8}\,, \tag{10}$$

where ∇_h is the horizontal Laplace operator and ν_h and ν_z are horizontal and vertical diffusion coefficients respectively, which are equal for velocity, potential temperature and the scalar. The forcing is restricted to the large scales and is purely horizontal and two-dimensional. It is designed in such a way that it generates a constant energy input P, as in Lindborg & Brethouwer (2007).

As we have argued, a simulation with a vertical mean gradient should produce the same type of spectra for ϕ and θ. We have confirmed this, by carrying out simulations with $\boldsymbol{G}$ in the vertical direction, using both identical and different initial conditions for ϕ and θ. In this paper, we present the results from simulations in which $\boldsymbol{G}$ is in the horizontal x-direction. The simulations enable us to determine to what degree passive scalar statistics, such as spectra and structure functions, are universal, i.e. independent of the mean scalar gradient direction. The simulation parameters are listed in table 1.

To assess the influence of rotation on scalar statistics we have carried out one simulation with rotation (run Ar). Lindborg (2005) showed that stratified turbulence with a forward energy cascade can prevail if the Rossby number $Ro < 0.1$. Here $Ro = P^{1/3}/l_h^{2/3} f_o$ with l_h the horizontal length scale at which the energy is injected. In run Ar $Ro = 0.3$.

3. Results

After an initial period of adjustment the flow field reaches a statistically stationary state in which the sum of the kinetic and potential energy dissipation is equal to the forcing input, and the kinetic and potential energy stay approximately constant. Through the nonlinear cascade process the energy which is injected at the large scales is transferred to small scales where it is dissipated. The velocity and potential temperature fields reach a statistical stationary state relatively fast. In run Ar also the scalar field becomes statistical stationary, but in run A and B the scalar variance continues to grow slowly, implying that the mean production of scalar variance, $2\langle \boldsymbol{G}\cdot\boldsymbol{u}\rangle$, is not exactly balanced by the mean dissipation, ε_θ. The computed dissipation-production ratios are 0.89 and 0.88 at the end of runs A and B respectively. The slow growth of the scalar variance is likely caused by the energy growth in the so-called shear mode with $k_h = 0$ in run A and B. This growth is inhibited by rotation in run Ar. Inertial range statistics are, however, not affected by the scalar variance growth because it takes place on very long time scales. In terms of an eddy turnover time $t_{eddy} = l_h^{2/3}/P^{1/3}$, run A is progressed till $t = 158t_{eddy}$ and run B till $t = 12t_{eddy}$. In the atmospheric mesoscale dynamics the eddy turnover time is of the order of one day (Lindborg 2006).

Figure 1 shows compensated horizontal one-dimensional spectra of the kinetic and potential energy extracted from the simulations. The imprint of the forcing of the modes $k_h \in [1, 3]$ is visible in the kinetic energy spectrum. For wave numbers between $k_h = 3$ and about 40 and 100 in run A/Ar and B respectively, the kinetic and potential energy spectra fall approximately on a straight horizontal line and display a $k_h^{-5/3}$-power-law range. We find that $C_K \simeq C_P \simeq 0.47$ in agreement with Lindborg (2006) and Lindborg & Brethouwer (2007). Figure 1 also displays the compensated horizontal one-dimensional spectra of the scalar variance. These are calculated as the mean of the two one-dimensional spectra in the x and y-directions. Just as the kinetic and potential energy spectra, the passive scalar spectra show a $k_h^{-5/3}$-power-law range. Moreover, the compensated passive scalar spectra approximately fall on top of the kinetic and potential energy spectra, implying that the Obukhov-Corrsin constant of stratified turbulence has the value $C_\theta \simeq 0.47$. Interestingly, this is close to the Obukhov-Corrsin constant observed in Kolmogorov turbulence (Sreenivasan 1996). The rotation appears to have a minor or insignificant influence on the inertial range spectra.

The passive scalar mean gradient introduces horizontal large-scale anisotropy in the scalar field but this does not lead to any observable differences in the two horizontal scalar spectra in the inertial range as shown in figure 2, which displays the ratio of the scalar variance spectra in the x and y-directions. This ratio is very close to unity in the inertial range, implying horizontal isotropy.

Figure 3 shows the scaled horizontal second-order passive scalar structure functions, $\langle \delta\theta\delta\theta \rangle / \varepsilon_\theta \varepsilon_K^{-1/3}$, from run A and B with $\boldsymbol{r}$ parallel to $\boldsymbol{G}$. The horizontal structure function with $\boldsymbol{r}$ perpendicular to $\boldsymbol{G}$ was almost indistinguishable from the structure function with $\boldsymbol{r}$ parallel to $\boldsymbol{G}$ in the inertial range, which again is a sign of horizontally isotropic dynamics. In run B, the second order structure function scales as $r^{2/3}$ between $r = 0.03$ and about 0.5 and also in run A we see such a $r^{2/3}$-range, although it is narrower. The computed constant C'_θ in (3) is 1.6 in run B and 1.9 in run A and this corresponds to $C_\theta \approx 0.25 C'_\theta \simeq 0.40$ and 0.48, respectively. These values are quite close to $C_\theta \simeq 0.47$ estimated from the scalar variance spectra. The deviations from the theoretical relation $C_\theta \approx 0.25 C'_\theta$ are due to the finite width of the inertial range. The second-order potential temperature structure functions extracted from run B also showed a clear $r^{2/3}$-scaling range (not shown here) from which we estimated $C_P \simeq 0.45$ which is close to the value estimated directly from the potential energy spectrum.

Intermittency theories for turbulence (Warhaft 2000) predict corrections to the Obukhov-Corrsin theory. According to such theories the passive scalar structure function of order n scales as $\langle \delta\theta^n \rangle \sim r^{\zeta_n}$, where the scaling exponent ζ_n deviates from $n/3$. In three-dimensional locally isotropic turbulence deviations indeed occur for $n \geq 3$ (Warhaft 2000). We have calculated the fourth-order horizontal passive scalar structure functions and observed that $\zeta_4 \simeq 1.15$, which is smaller than the Obukhov-Corrsin theory prediction $\zeta_4 = 4/3$. The calculated fourth-order potential temperature structure functions showed similar scaling exponents whereas the fourth-order velocity structure functions did not display a clear scaling range.

The flatness factor of the passive scalar difference $\delta\theta$ is defined as

$$F = \frac{\langle \delta\theta^4 \rangle}{\langle \delta\theta\delta\theta \rangle^2} \,. \tag{11}$$

It is displayed in figure 4 together with the flatness factors of the potential temperature and longitudinal velocity difference. According to the Obukhov-Corrsin theory, F should be constant in the inertial range. In our simulations F is not constant but grows for decreasing r, indicating a growing intermittency as the scales become smaller. The passive scalar flatness factor is proportional to $r^{-0.2}$ in the inertial range in run A and B, and proportional to $r^{-0.4}$ in run Ar. In all runs, the flatness factors of the potential temperature and the velocity is also proportional to $r^{-0.2}$ (the results from run Ar are very similar to run A and not shown here). At small separations F is of the order 10, which is a sign of intermittent high amplitude events in the small-scale turbulent field. In all simulations, the flatness factor of the scalar is larger than the flatness factors of the potential temperature and velocity. In the latter two cases F approaches the Gaussian value 3 at large r whereas for the scalar it does not in run A and B. This indicates a stronger intermittency in the scalar field than in the potential temperature and velocity fields. Measurements in the atmospheric boundary layer show that the flatness factor of the velocity scales as $r^{-0.12}$ in the inertial range (Dhruva *et al.* 1997), but in the middle atmosphere F grows much faster with decreasing scales (Lindborg 1999) revealing a much stronger intermittency than in our simulations.

We conclude that the results of the numerical simulations are consistent with predictions made on basis of stratified turbulence theory, according to which the horizontal spectra and structure functions of passive scalar variance have the same form as in the Obukhov-Corrsin theory for locally isotropic turbulence. It is, however, important to realise that the dynamics of stratified turbulence is radically different from classical isotropic turbulence. The stratified turbulence we have simulated here is extremely anisotropic, with vertical to horizontal length scale aspect ratios of $\mathcal{O}(0.01)$. The simulation results are also consistent with atmospheric observations. Our study suggests that measured passive scalar mesoscale range spectra in the middle atmosphere can be explained by the presence of stratified turbulence at these scales.

References

Bacmeister, J T, Eckermann, S D, Newman, P A, Chan, K R, Loewenstein, M, Proffitt, M H, Gary, B L (1996) Stratospheric horizontal wavenumber spectra of winds, potential temperature, and atmospheric tracers observed by high-altitude aircraft. *J. Geophys. Res.* **101**, 9441–9470.

Billant, P, Chomaz, J-M (2001) Self-similarity of strongly stratified inviscid flows. *Phys. Fluids* **13**, 1645–1651.

Brethouwer G, Billant P, Lindborg E, Chomaz J-M (2007) Scaling analysis and simulation of strongly stratified turbulent flows. *J. Fluid Mech.* **585**, 343–368.

Cho, J Y N, Zhu, Y, Newell, R E, Anderson, B E, Barrick, J D, Gregory, G L, Sachse, G W, Carroll, M A, Albercook, G M (1999) Horizontal wavenumber spectra of winds, temperature, and trace gases during the Pacific Exploratory Missions: 1. Climatology. *J. Geophys. Res.* **104**, 5697–5716.

Dhruva, B, Tsuji, Y, Sreenivasan, K R (1997) Transverse structure functions in high-Reynolds-number turbulence. *Phys. Rev. E* **56**, 4928–4930.

Lindborg E (1999) Can the atmospheric kinetic energy spectrum be explained by two-dimensional turbulence? *J. Fluid Mech.* **388**, 259–288.

Lindborg, E (2005) The effect of rotation on the mesoscale energy cascade in the free atmosphere. *Geophys. Res. Lett.* **32**, L01809.

Lindborg E (2006) The energy cascade in a strongly stratified fluid. *J. Fluid Mech.* **550**, 207–242.

Lindborg E, Brethouwer G (2007) Stratified turbulence forced in rotational and divergent modes. *J. Fluid Mech.* **586**, 83–108.

Lindborg E, Cho, J Y N (2000) Determining the cascade of passive scalar variance in the lower stratosphere. *Phys. Rev. Lett.* **85**, 5663–5666.

Nastrom, G D, Gage, K S (1985) A climatology of atmospheric wavenumber spectra of wind and temperature observed by commercial aircraft. *J. Atmos. Sci.* **42**, 950–960.

Nastrom, G D, Jasperson, W H, Gage, K S (1986) Horizontal spectra of atmospheric tracers measured during the global atmospheric sampling program. *J. Geophys. Res.* **91**, 13201–13211.

Riley, J J, deBruynKops, S M (2003) Dynamics of turbulence strongly influenced by buoyancy. *Phys. Fluids* **15**, 2047–2059.

Sparling, L C, Bacmeister, J T (2001) Scale dependence of tracer microstructure: PDFs, intermittency and the dissipation scale. *Geophys. Res. Lett.* **28**, 2823–2826.

Sreenivasan, K (1996) The passive scalar spectrum and the Obukhov-Corrsin constant. *Phys. Fluids* **8**, 189–196.

Strahan, S E, Mahlman, J D (1994) Evaluation of the SKYHI general circulation model using aircraft N_2O measurements. 2. Tracer variability and diabatic meridional circulation. *J. Geophys. Res.* **99**, 10319–10332.

Tjemkes, S A, Visser, M (1994) Horizontal variability of temperature, specific humidity, and cloud liquid water as derived from spaceborne observations. *J. Geophys. Res.* **99**, 23089–23105.

Warhaft, Z (2000) Passive scalars in turbulent flows. *Annu. Rev. Fluid Mech.* **32**, 203–240.

Run	A	Ar	B
F_h	2.5×10^{-3}	2.5×10^{-3}	5.8×10^{-4}
L_x/L_z	40	40	256
$L_z N/\sqrt{E_K}$	29.8	27.5	19.8
$N_x \times N_z$	384×96	384×96	1024×128
ν_h	8.0×10^{-15}	8.0×10^{-15}	7.2×10^{-18}
ν_v	3.7×10^{-22}	3.7×10^{-22}	6.5×10^{-29}
$\varepsilon_P/\varepsilon_K$	0.32	0.39	0.31

Table 1. Overview of the numerical and physical parameters used in the simulations. N_x and N_z are the number of modes in the horizontal respectively vertical direction. The ratio of the vertical grid spacing and Ozmidov length scale $\varepsilon_K^{1/2}/N^{3/2}$ is 7.1 in all simulations.

Figure 1. Compensated horizontal one-dimensional kinetic energy spectra $E_K(k_h)k_h^{5/3}/\varepsilon_K^{2/3}$, potential energy spectra $E_P(k_h)k_h^{5/3}\varepsilon_K^{1/3}/\varepsilon_P$ and passive scalar variance spectra $E_\theta(k_h)k_h^{5/3}\varepsilon_K^{1/3}/\varepsilon_\theta$. The straight line is $C = 0.47$. (a), run A; (b), run Ar; (c), run B.

Figure 2. Ratio of the horizontal scalar variance spectra with k_h parallel to the mean scalar gradient and perpendicular.

Figure 3. Scaled second-order structure function of the passive scalar $\langle \delta\theta \delta\theta \rangle / \varepsilon_\theta \varepsilon_K^{-1/3}$ with $\boldsymbol{r}$ horizontal and parallel to the mean scalar gradient.

Figure 4. Flatness factors of the longitudinal velocity differences $F(\delta u)$, potential temperature $F(\delta\phi)$ and the scalar with $\boldsymbol{r}$ parallel to $\boldsymbol{G}$, $F(\delta\theta)$.

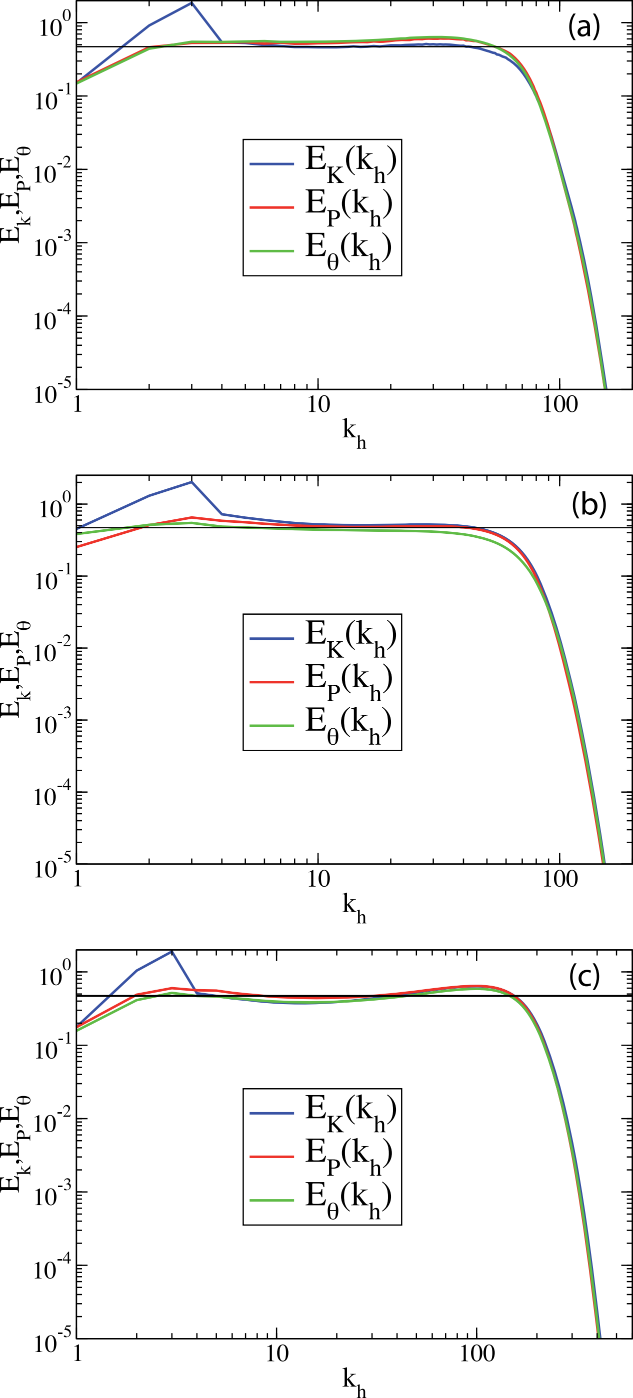
(a)
$E_K(k_h)$
$E_P(k_h)$
$E_\theta(k_h)$
E_k, E_P, E_θ
k_h
(b)
$E_K(k_h)$
$E_P(k_h)$
$E_\theta(k_h)$
E_k, E_P, E_θ
k_h
(c)
$E_K(k_h)$
$E_P(k_h)$
$E_\theta(k_h)$
E_k, E_P, E_θ
k_h

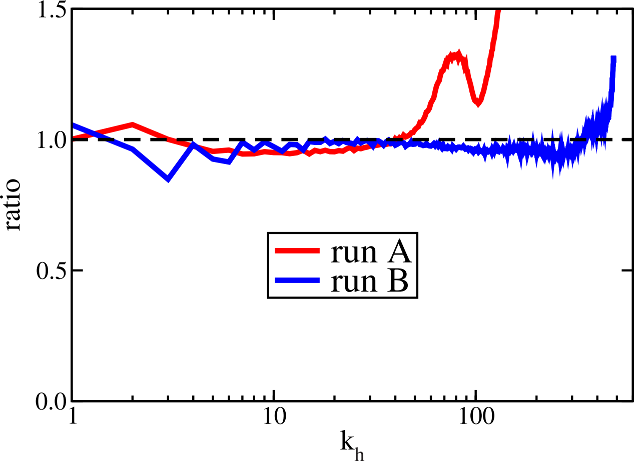
1.5
1.0
0.5
0.0
ratio
run A
run B
1
10
100
k_h

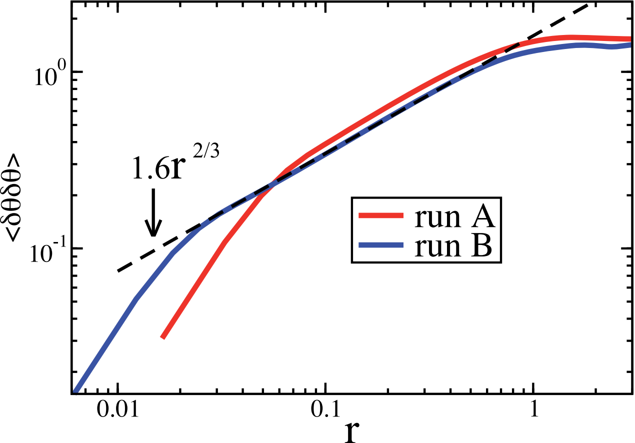

1.6r $^{2/3}$
run A
run B
<δθδθ>
r
10^{0}
10^{-1}
0.01
0.1
1

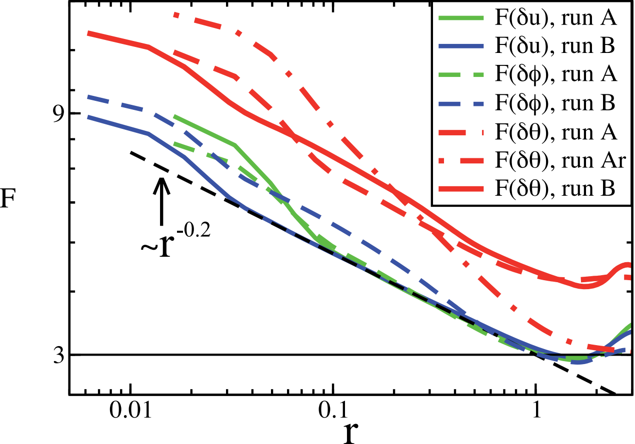

F(δu), run A
F(δu), run B
F(δφ), run A
F(δφ), run B
F(δθ), run A
F(δθ), run Ar
F(δθ), run B
~r^{-0.2}
F
9
3
0.01
0.1
1
r